



Time-variations of the regional evapotranspiration rate from GRACE satellite gravimetry

Guillaume Ramillien, Frédéric Frappart, Andreas Güntner, Thanh Ngo-Duc,
Anny Cazenave, Katia Laval

► To cite this version:

Guillaume Ramillien, Frédéric Frappart, Andreas Güntner, Thanh Ngo-Duc, Anny Cazenave, et al.. Time-variations of the regional evapotranspiration rate from GRACE satellite gravimetry. *Water Resources Research*, American Geophysical Union, 2006, 42, pp.W10403. <10.1029/2005WR004331>. <hal-00429435>

HAL Id: hal-00429435

<https://hal.archives-ouvertes.fr/hal-00429435>

Submitted on 2 Nov 2009

HAL is a multi-disciplinary open access archive for the deposit and dissemination of scientific research documents, whether they are published or not. The documents may come from teaching and research institutions in France or abroad, or from public or private research centers.

L'archive ouverte pluridisciplinaire **HAL**, est destinée au dépôt et à la diffusion de documents scientifiques de niveau recherche, publiés ou non, émanant des établissements d'enseignement et de recherche français ou étrangers, des laboratoires publics ou privés.

Time-variations of the regional evapotranspiration rate from GRACE satellite gravimetry

G. Ramillien¹, F. Frappart^{1,2}, A. Güntner³, T. Ngo-Duc⁴, A. Cazenave¹ and K. Laval⁴

¹ LEGOS, UMR5566, CNRS/CNES/IRD/UPS, Observatoire Midi-Pyrénées, Toulouse, France

² LMTG, UMR5572, CNRS/IRD, UPS, Toulouse, France

³ GeoForschungZentrum (GFZ), Telegrafenberg, Potsdam, Germany

⁴ IPSL/Laboratoire de Météorologie Dynamique (LMD), Paris, France

Revised version for *Water Resources Research*, April 2006

Corresponding address:

G. Ramillien

GOHS, LEGOS UMR5566 - OMP

18, Avenue Edouard Belin

31400 Toulouse, France

Tel: (+33) 05 61 33 29 34

e-mail: ramillie@notos.cst.cnes.fr

Abstract

Since its launch in March 2002, the GRACE mission is measuring the global time variations of the Earth's gravity field with a current resolution of ~500 km. Especially over the continents, these measurements represent the integrated land water mass including surface waters (lakes, wetlands and rivers), soil moisture, groundwater and snow cover. In this study, we use the GRACE land water solutions computed by Ramillien et al. (2005a) through an iterative inversion of monthly geoids from April 2002 to May 2004, to estimate time-series of basin-scale regional evapotranspiration rate -and associated uncertainties-. Evapotranspiration is determined by integrating and solving the water mass balance equation, which relates land water storage (from GRACE), precipitation data (from the Global Precipitation Climatology Centre), runoff (from a global land surface model) and evapotranspiration (the unknown). We further examine the sensibility of the computation when using different model runoff. Evapotranspiration results are compared to outputs of four different global land surface models. The overall satisfactory agreement between GRACE-derived and model-based evapotranspiration prove the ability of GRACE to provide realistic estimates of this parameter.

1. Introduction

Temporal change of evapotranspiration (ET) provides precious indications of the global water cycle and climate change, as well as important boundary conditions for climate models. Unfortunately, there are no global-scale in situ measurements of ET. Algorithms for deriving ET from the raw satellite observations require location-specific calibration, making them very difficult to apply globally. In global Land Surface Models (LSMs), ET is modelled through different empirical approaches, e.g., using the Penman equation (De Marsily, 1981), through parameterization of the latent heat flux (Ducoudré et al., 1993, Milly and Shmakin, 2002) according to the bulk equation introduced by Monteith (1963), etc. At large scales, the temporal distribution of ET is a function of climatic conditions, soil moisture availability, the vegetation type as well as the area of the surface water (wetlands and rivers). These surface conditions are poorly known for global scale modelling. Existing models provide substantially dissimilar estimates at monthly, seasonal and even annual time scales (Verant et al., 2004).

Recent results of the total land water storage based on the GRACE (Gravity Recovery and Climate Experiment) space mission (Tapley et al., 2004; Wahr et al., 2004; Schmidt et al., 2005, Ramillien et al., 2005a) suggest that the variations of continental water storage are mainly seasonal and the largest amplitudes are located in the large tropical basins of Africa

and South America, in the South East Asia during monsoon events, as well as in the high-latitude regions of the Northern hemisphere due to the snow. These patterns are consistent with those provided by global LSMs, such as the Water GAP Global Hydrology Model (WGHM; Döll et al., 2003), the Land Dynamics model (LaD; Milly and Shmakin, 2002), the Global Land Data Assimilation System (GLDAS; Rodell et al., 2004a) and the Organizing Carbon and Hydrology In Dynamics EcosystEms model (ORCHIDEE; Verant et al., 2004). Rodell et al. (2004b) computed time-series of ET over the Mississippi River basin, using the land water information from the monthly GRACE geoids combined with precipitation and runoff data. Rodell et al. (2004b) showed that the GRACE-derived ET is comparable to the estimates provided by the ECMWF (European Center for Medium range Weather Forecasting) reanalysis and the GLDAS models.

In this paper, we compute time variations of basin-scale ET rates (and associated uncertainties) by time integrating, and then solving, the water mass balance equation, using land water solutions derived from GRACE (Ramillien et al., 2005a) and independent information on precipitation and runoff. We present estimates of ET, and associated errors, for sixteen drainage basins from April 2002 up to May 2004. For validation, we compare the ET estimates with predictions from global LSMs.

2. Method of analysis

Water mass balance equation

For a given watershed, the instantaneous equation of the water mass balance is:

$$P = \frac{\partial W}{\partial t} + ET + R \quad (1)$$

where P , $\frac{\partial W}{\partial t}$, R are precipitation, water mass storage and runoff respectively. These terms are generally expressed in terms of water mass (mm of equivalent-water height) or pressure (kg/m^2) per day. Time integration of Eq.1 between times t_1 and t_2 (the starting and the ending dates of the considered period, with $\Delta t = t_2 - t_1$, assumed to be ~ 30 day, the average time span over which the GRACE geoids are provided) gives:

$$\Delta ET = \frac{1}{\Delta t} [\Delta P - \Delta R - \Delta W] \quad (2)$$

In Eq.2 above, ET is mm/day. If we have high-frequency sampled data (e.g., daily data for precipitation), the classical method of the “rectangle” summation has been applied to integrate precipitation P and runoff R over the Δt time interval. ΔW is the variation of the water mass

inside the drainage basin area between t_1 and t_2 . This term is directly computed as the difference between two monthly GRACE solutions:

$$\Delta W = W(t_2) - W(t_1) \quad (3)$$

The GRACE-based land water solutions computed in Ramillien et al. (2005) are spherical harmonics of a surface density function $F(\theta, \lambda, k)$ that represents the global map of W :

$$F(\theta, \lambda, k) = \sum_{n=1}^N \sum_{m=0}^n [C_{nm}^F(k) \cos(m\lambda) + S_{nm}^F(k) \sin(m\lambda)] \tilde{P}_{nm}(\cos \theta) \quad (4)$$

In Eq.4, θ and λ are co-latitude and longitude, k is a given monthly solution. n and m are degree and order, \tilde{P}_{nm} is the associated Legendre function, and $C_{nm}^F(t)$ and $S_{nm}^F(t)$ are the normalized coefficients of the decomposition. In practice, the spherical harmonic development cutoff N used for the land water solutions in Ramillien et al. (2005) is limited to degree 30. This corresponds to a spatial resolution of 660 km.

Instead of using the “time-piece wise” approach proposed earlier by Rodell et al. (2004b) that requires high-frequency data (and those were not available) to evaluate Eq.3, we linearly approximate the water mass variations of month ‘ k ’ as:

$$\Delta W_k \approx \frac{1}{2} (\delta W_{k+1} - \delta W_{k-1}) \quad (5)$$

Missing monthly land water solutions data (due to the lack of GRACE geoids) are simply interpolated from the previous and the next months.

Precipitation and runoff data are provided as monthly grids of $1^\circ \times 1^\circ$ (see section 3). Thus to be consistent with the land water solutions, we develop gridded P and R data into spherical harmonics, low-pass filter at degree 30 and re-compute gridded data using Eq. 4.

Sixteen river basins are considered in this study. Their location is shown in Fig.1. The contour of each basin is based on a mask of 0.5° resolution from Oki and Sud (1998). For each month ‘ k ’, gridded ΔP , ΔR , and ΔW are spatially averaged over each river basin according to:

$$\bar{F}_k = \frac{R_e^2}{S} \sum_{j \in S} F(\theta_j, \lambda_j, k) \delta \lambda \delta \theta \sin \theta_j \quad (6)$$

where F_k represents ΔP , ΔR or ΔW . $\delta \lambda$ and $\delta \theta$ are grid steps in longitude and latitude respectively (generally $\delta \lambda = \delta \theta$), and R_e is mean Earth’s radius (~ 6378 km).

Once each quantity is averaged spatially, it is easy to compute mean ET using Eq.2. Monthly ET values were further divided by a factor of 30 to convert the unit of mm/month into mm/day.

As Eq.2 is linear and neglecting interpolation errors in Eq.5, one can easily compute associated absolute errors from the relative uncertainties ε_P and ε_R on P and R respectively:

$$\sigma_{ET} \approx \varepsilon_P \Delta P + \varepsilon_R \Delta R + 2 \frac{\bar{\sigma}_w}{\Delta t} \quad (7)$$

σ_w is the total error for a single month GRACE solution. Relative uncertainty on precipitation fields ε_P is assumed $\sim 11\%$ (Rodell et al., 2004b). However, modelled runoff data are much more uncertain, especially in large low-land watersheds such as the Amazon basin. In situ measurements of Amazon discharges by 30%: observed annual averages are 155,000 m³/s (Vörösmarty et al., 1996), and 170,000-200,000 m³/s (Dunne et al., 1998; Mertes et al., 1996; Meade et al., 1991).

Regional runoff from different models, even for well-constrained regions like in the US, can vary up to a factor of four (Lohmann et al., 2004). This suggests the situation must be worse elsewhere. Thus, we considered as realistic values for ε_R of $\sim 30\%$.

Wahr et al., (2004) estimated σ_w to be ~ 18 mm for a 750-km spatial average GRACE-based land water solutions. Ramillien et al. (2005b) found $\sigma_w \sim 15$ mm the final *a posteriori* uncertainties on the land water solutions, with spatial resolution of 660 km. As we use a geographical mask to average the land water signal over each basin, $\bar{\sigma}_w < 1$ mm. Thus, for each monthly estimate, the contribution of the land water to the total budget error (Eq.7) should be no much than 0.07 mm/day.

3. Data used in this study

3.1 The land water solutions estimated from GRACE

As explained above, here we use the land water solutions presented in Ramillien et al. (2005). These solutions range from April 2002 to May (2004), with a few missing months. They consist of total land water mass (surface waters: rivers, lakes, flood plains; soil moisture; groundwater; snow). Their spatial resolution is 660 km. Associated *a posteriori* uncertainties are also provided

3.2 Other data sets used in this study for the period 2002-2004

3.2.1 Precipitation data

We use the monthly Global Precipitation Climatology Centre (GPCC) products (Rudolf et al., 1994). These are gridded data sets based on raingauge observations, which have been checked using a high level quality control system (Rudolf et al., 2003). We used the products with the 1° by 1° geographical latitude and longitude resolution that contain monthly precipitation totals (mm/month) derived from records of 30,000 to 40,000 gauge stations.

3.2.2 Runoff data

For runoff, we use the predicted values from two LSMs : the WGHM model (Döll et al., 2003) and the LaD model (Milly and Shmakin, 2002).

Runoff from WGHM

WGHM was specifically designed to estimate river discharge for water resources assessments. It computes 0.5°x0.5° gridded time series of monthly runoff and river discharge and is tuned against time series of annual rivers discharges measured at 724 globally distributed stations. Surface runoff is computed from the water balance equation that takes into account the water content within the effective root zone, the effective precipitation and the ET. This vertical water balance of the land and open water fraction of each cell is coupled to a lateral transport scheme, which routes the runoff through series of storages within the cell and then transfers the resulting cell outflow to the downstream cell. It is assumed that surface/subsurface runoff is routed to surface storage without delay. Other products of the model are monthly gridded time series of snow depth, soil water within the root zone, ground water and surface water storage in rivers, lakes and wetlands, ET.

Runoff from LaD

The LaD model (Milly and Shmakin, 2002) provides monthly 1° x 1° gridded time series of surface parameters. For each cell of the model, the total water storage is composed of three stores: a snowpack store, a root-zone store and a groundwater store and the total energy storage is equal to the sum of latent heat of fusion of the snowpack and the glacier and sensible heat content. Runoff generation in the LaD model is essentially a soil-store-excess mechanism, with no limitation on infiltration capacity (Milly et al., 2002), according to the Manabe's simple model (Manabe, 1969). Root-zone water does not exceed a specified maximum amount (i.e., the field capacity). This simplified scheme for modelling runoff assumes instantaneous downstream flow of all runoff, so that surface water storage is

neglected. Discharge past any point on the river corresponds to the summation over all upstream cells of the product of runoff rate and cell area at that time.

3.3 ET predictions from four different land surface models

GRACE-derived ET is compared to predictions from four global LSMs . We present below how this hydrological parameter is computed by these models.

3.3.1 ET predictions from WGHM

In WGHM, ET is computed as a function of potential ET (the difference between the maximum potential ET and the canopy transpiration), the soil water content in the effective root zone and the total available soil capacity as:

$$ET = \min\left(E_{pot} - E_c, (E_{pot\ max} - E_c) \frac{S_s}{S_{s\ max}}\right) \quad (9)$$

where E_{pot} is potential ET (mm/day), E_c is evaporation from the canopy (mm/day), $E_{pot\ max}$ is maximum potential ET (mm/day), S_s is soil water content within the effective root zone (mm), $S_{s\ max}$ is total available soil water capacity within the effective root zone (mm). In this latter equation, canopy evapotranspiration has to be added. These $1^\circ \times 1^\circ$ (originally $0.5^\circ \times 0.5^\circ$) gridded monthly data are available for 2002 to 2004.

3.3.2 ET predictions from LaD

In the LaD model, ET is parameterized as:

$$ET = \frac{\rho_a}{r_a + r_s} (q_s(T_0) - q_a) \min\left(\frac{W_R}{0.75W_R^*}, 1\right) \quad (10)$$

where: ρ_a is the density of the air, r_a is the aerodynamic resistance for scalar transfer, r_s is a bulk stomatal resistance under conditions of negligible water stress, $q_s(T_0)$ is the mixing ratio of water vapour associated with saturated conditions at the surface temperature, q_a is the mixing ratio at a given level in the atmospheric surface layer, W_R is the water storage in the root-zone store, W_R^* is the maximum possible value of W_R . The final factor in Eq.10 accounts for the limitation of ET by water stress. The LaD ET are provided from January 1980 to April 2004 .

3.3.3. ET predictions from GLDAS

The GLDAS project is led by scientists of the National Aeronautics and Space Administration (NASA) and the National Oceanic and Atmospheric Administration (NOAA) in association with researchers of the Princeton University, the University of Washington and the Weather Service Office of Hydrology (Rodell et al., 2004a). Princeton, Washington and OHD participated in North American LDAS project but not GLDAS. This uncoupled land surface assimilation scheme, used for climate studies, is forced by real time outputs of the NCEP (National Centres for Environmental Prediction) reanalysis, satellite data and radar precipitation measurements. Parameters are deduced from high-resolution vegetation, soil coverage and ground elevation data. Data assimilation is performed by one-dimensional Kalman filtering strategy to produce optimal fields of surface parameters. Nominal spatial and temporal resolutions of the grids are 0.25 degree and 3 hours respectively, and all fields are defined for all lands north of 60°S. Outputs used in this study were from a 1° resolution simulation of Noah land surface model (GLDAS/Noah) in which data assimilation was not applied. Monthly 1°x1° means of the ET rates (units: kg/m²) were interpolated from these nominal 3-hour outputs. Due to problems of simulation in the ET subroutine of GLDAS, the ET rate fields after 10/2002 were computed as the ratio of the predicted latent heat flux and the constant latent heat of evaporation (around 2.501 10⁶ J/kg) (M. Rodell, *personal communication*).

3.3.4 ET predictions from ORCHIDEE

The ORCHIDEE land surface model (Verant et al., 2004; Krinner et al., 2005), developed at the Institut Pierre Simon Laplace (Paris, France), provides monthly 1° x 1° gridded time series of surface parameters estimated from 1948 to 2003. For this study, we only use the ET output of SECHIBA (Schématisation des Echanges Hydriques l'Interface entre la Biosphère et l'Atmosphère) (Ducoudré et al., 1993; De Rosnay and Polcher, 1998), which is the water and energy cycle component of ORCHIDEE. In SECHIBA, the ET flux is described using the bulk equation introduced by Monteith (1963), similar to Eq.10.

4. Results

Figure 2 a-b presents GRACE-based ET time series for each of the 16 selected river basins. The ET estimates presented in Fig.2 use the WGHM runoff for the computations. For comparison, are also plotted model-based ET (from WGHM, GLDAS, LaD and ORCHIDEE). In view of the short time span considered here, the signal is dominated by the seasonal signal. Maximum of the ET seasonal cycle occur in July for Northern hemisphere

river basins and in January in the Southern hemisphere. These are in the range 3-4 mm/day for all basins (at the spatial resolution of ~660 km). These GRACE-based ET seasonal variations are consistent with model predictions as well as observations. In the central Amazon basin for example, a 3.6 mm/day seasonal amplitude was found by Costa et al. (1999).

Table 1 presents the results of statistical comparisons between GRACE-derived and model-based ET. The rms (i.e., root-mean squares) differences are averaged over the overlapping months over the 2002-2004 period. In general, rms differences between GRACE-based and model-based ET are less than 1 mm/day, except for the Brahmaputra watershed, a relatively small basin, where rms differences range from 1.46 to 1.65 mm/day. The lowest rms difference is found with the ORCHIDEE model over the Mississippi basin (~0.29 mm/day rms). This result for the Mississippi basin is comparable with that from Rodell et al. (2004b). These authors derived a time-series of the ET rate changes by low-pass filtering the GRACE geoids according to the Wahr et al., (1998) method. They also found a good agreement with the GLDAS model for monthly means (~0.83 mm/day rms) (spatial resolution of 750 km). As this basin is well-covered by field observations, this comparison confirms the great value of GRACE for estimation ET.

In order to test the impact of the R model values to compute ET (and associated uncertainties), we consider two different river basin cases: the Amazon basin which suffers from lack of observations (we then assume the model error is large in this region), and the Mississippi basin which is well-covered by in situ data (thus error on R should be small).

We present in Fig. 3 a-b GRACE-based ET values using monthly runoff data from two different models (WGHM and LaD). As seen on Fig.3 a-b, considering LaD runoff produces higher ET than using WGHM runoff: the mean difference between WGHM and LaD curves is a constant bias over the considered time span (1.5 mm/day and 0.40 mm/day for Amazon and Mississippi basins respectively). Besides, the ET rate obtained by using WGHM runoff remains the closest to the mean value proposed by Costa et al. (1999) for the Amazon River basin.

Figure 4 a-b presents ET uncertainties (Eq.7) for the two basins (Amazon and Mississippi). As expected by the accuracy of the model runoff in these two regions, extreme errors (1.8 mm/day, ~50% relative error) are found in the Amazon basin. In the case of the Mississippi basin, the maximum error reaches ~0.55 mm/day (around June 2003) that corresponds to 20% of the amplitude of ET rate. Accuracy of the ET rate estimates should be clearly improved when the quality of the input runoff data from models increases.

7. Summary

In this study, we have developed an approach based on the resolution of the water mass balance equation to derive regional time variations of the ET rate based on GRACE data. We also estimate associated absolute errors associated with the GRACE-based ET time series, from the relative uncertainties on precipitation and runoff. These absolute errors reach up to 1/6 of the seasonal amplitudes of the estimated ET. Comparison of the GRACE-based ET with different global LSMs ET estimates shows good overall agreement, especially at the seasonal time scale.

In the future, new GRACE land water solutions would be considered as input to the proposed approach to complete the series of ET rate variations. New perspectives of ET rate detection from space gravimetry would give access to further surface information such as vegetation distribution and soil type.

Acknowledgements

We would like to thank Petra Döll, Chris Milly, Matthew Rodell, for having made the monthly outputs of their models available to us. This work was partly funded by the French Programme National de Télédétection Spatiale (PNTS). One of us (FF) benefited from a CNES-ALCATEL SPACE PhD grant.

References

- Costa M. H. and J. A. Foley, 1999, "Trends in the hydrologic cycle of the Amazon basin", *J. Geophys. Res.*, 104, 14189-14198.
- De Marsily G., 1981, **Hydrologie quantitative**, Ed. Masson, Paris, In French, ISBN: 2-225-75504-3, 217 pp.
- De Rosnay P. and J. Polcher, 1998, "Modeling root water uptake in a complex land surface scheme coupled to a GCM", *Hydrology and Earth System Sciences*, 2(2-3), 239-256.
- Döll P., F. Kaspar and B. Lehner, 2003, "A global hydrological model for deriving water availability indicators: model tuning and validation", *J. Hydrol.*, 270, 105-134.

Ducoudré N., K. Laval and A. Perrier, 1993, "SECHIBA: a new set of parametrization of the hydrologic exchanges at the land/atmosphere interface within the LMD atmosphere general circulation model", *J. Climate*, 6 (2), 248-273.

Dunne T., L. A. K. Mertes, R. H. Meade, J. E. Richey and B. R. Forsberg, 1998, "Exchanges of sediment between the flood plain and channel of Amazon River in Brazil", *GSA Bulletin* 110, 450-467.

Krinner G., N. Viovy, N. De-Noblet-Ducoudré, J. Ogée, J. Polcher, P. Friedlingstein, P. Ciais, S. Sitch and C. Prentice, 2005, "A dynamic global vegetation model for studies of the coupled atmosphere-biosphere system", *Global Change Biology*, 19, GB1015, doi: 10.1029/2003GB002199.

Lohmann D., K. E. Mitchell, P. R. Houser, E.F. Wood, J. C. Schaake, A. Robock, B. A. Cosgrove, J. Sheffield, Q. Duan, L. Luo, R. W. Higgins, R. T. Pinker and J. D. Tarpley, 2004, "Streamflow and water balance intercomparisons of four land surface models in the North American Land Data Assimilation System project", *J. Geophys. Res.*, 109, D7, D07S91, doi: 10.1029/2003JD003517.

Manabe S., 1969, "Climate and ocean circulation. 1. The atmospheric circulation and the hydrology of the Earth's surface", *Mon. Wea. Rev.*, 97, 739-774.

Meade R. H., J. M. Rayol, S. C. Da Conceicao and J. R. G. Natividade, 1991, "Backwater effects in the Amazon River basin of Brazil", *Environ. Geol. Water Sci.*, 18, 105-114.

Mertes L. A. K., T. Dunne and L. A. Martinelli, 1996, "Channel-floodplain geomorphology along the Solimões-Amazon River, Brazil", *GSA Bulletin*, 108, 1089-1107.

Milly P. C. D. and A. B. Shmakin, 2002, "Global modelling of land water and energy balances: 1. The Land Dynamics (LaD) model", *J. Hydrometeorol.*, 3, 283-299.

Monteith J. L., 1963, "Gas exchange in plant communities", *Environmental Control of Plant Growth*, L. T. Evans, Ed. Academic Press, 95-112.

Oki T. and Y. C. Sud, 1998, "Design of total runoff integrating pathways (TRIP) – A global river channel network", *Earth Interactions*, 2(1), 1-37.

Ramillien G., 2002, "Gravity/magnetic potential of uneven shell topography", *J. of Geodesy*, 76, 3, ISSN: 0949-7714, 139-149.

Ramillien G., A. Cazenave and O. Brunau, 2004, "Global time variations of hydrological signals from GRACE satellite gravimetry", *Geophys. J. Int.*, 158, 813-826.

Ramillien G., F. Frappart, A. Cazenave and A. Güntner, 2005a, "Time variations of the land water storage from an inversion of 2 years of GRACE geoids", *Earth Plan. Sci. Lett.*, 235, 283-301.

Ramillien G., A. Cazenave, Ch. Reigber, R. Schmidt and P. Schwintzer, 2005b, "Recovery of global time variations of surface water mass by GRACE geoid inversion", *IAG meeting Proceedings*, Springer-Verlag, Porto, Portugal.

Rodell M. and J. S. Famiglietti, 1999, "Detectability of variations in continental water storage from satellite observations of the time dependent gravity field", *Water Resour. Res.*, 35, 2705-2723.

Rodell M. et al., 2004a, "The Global Land Data Assimilation System", *Bull. Am. Meteorol. Soc.*, 85, 381-394.

Rodell M., J. S. Famiglietti, J. Chen, S. I. Seneviratne, P. Viterbo, S. Holl and C. R. Wilson, 2004b, "Basin scale estimate of evapotranspiration using GRACE and other observations", *Geophys. Res. Lett.*, 31, L20504, doi: 10.1029/2004GL020873.

Rudolf, B., H. Hauschild, W. Rueth and U. Schneider, *Terrestrial Precipitation Analysis: Operational Method and Required Density of Point Measurements*. In: *Global Precipitations and Climate Change* (Ed. M. Desbois, F. Desalmond), NATO ASI Series I, Vol. 26, Springer-Verlag, p. 173-186, 1994.

Rudolf, B., T. Fuchs, U. Schneider and A. Meyer-Christoffer, Introduction of the Global Precipitation Climatology Centre (GPCC), Deutscher Wetterdienst, Offenbach a.M.; pp. 16., 2003.

Schmidt R., F. Flechtner, Ch. Reigber, P. Schwintzer, A. Güntner, P. Döll, G. Ramillien, A. Cazenave, S. Petrovic, H. Jochman and J. Wunsch, 2005, "GRACE observations of changes in continental water storage", *Glob. And Plan. Change*, in press.

Tapley B. D., S. Bettadpur, M. Watkins and Ch. Reigber, 2004, "The Gravity Recovery and Climate Experiment: mission overview and early results", *Geophys. Res. Lett.*, L09607, doi: 10.1029/2004GL019920.

Verant S., K. Laval, J. Polcher and M. Castro, 2004, "Sensitivity of the continental hydrological cycle to spatial resolution over the Iberian Peninsula", *J. of Hydrometeo.*, 5(2), 267-285.

Vörösmarty C. J., C. J. Willmott, B. J. Choudhury, A. L. Schloss, T. K. Stearns, S. M. Robeson and T. J. Dorman, 1996, "Analyzing the discharge regime of a large tropical river through remote sensing, ground-based climatic data, and modelling", *Water Resour. Res.*, 32, 3137-3150.

Wahr J., M. Molenaar and F. Bryan, 1998, "Time-variability of the Earth's gravity field: hydrological and oceanic effects and their possible detection using GRACE", *J. Geophys. Res.*, 103, 30,205-30,230.

Wahr J., S. Swenson, V. Zlotnicki and I. Velicogna, 2004, "Time-variable gravity from GRACE: first results", *Geophys. Res. Lett.*, 31, L11501, doi: 10.1029/2004GL019779.

Table 1

Statistical comparisons between the time series of the GRACE-based ET rate (this study) and the ET rate values provided by four global land surface models (GLDAS, LaD, ORCHIDEE, WGHM) for each studied basin: bias (on the upper part) and rms (root-mean square) differences (middle part) (units: mm/day). Comparisons for Amazon (in italic) and Mississippi basins (bottom part) using different runoff data as input (WGHM and LaD).

| Basin | GRACE vs. | | | |
|-------------|-----------|-------|----------|-------|
| | GLDAS | LaD | ORCHIDEE | WGHM |
| Amazon | 0,23 | -0,31 | 0,5 | 0,37 |
| Amur | -0,13 | -0,15 | 0,36 | 0,09 |
| Brahmaputra | 0,32 | -0,37 | 0,7 | 0,21 |
| Congo | 0,02 | -0,48 | 0,33 | 1,77 |
| Danube | -0,09 | -0,26 | 0,39 | 0,38 |
| Ganges | -0,11 | -0,64 | 0,01 | 0,07 |
| Hwang Ho | -0,03 | -0,43 | 0,09 | 0,06 |
| Mekong | 0,08 | -0,68 | 0,43 | 0,09 |
| Mississippi | -0,16 | -0,59 | 0,25 | 0,07 |
| Niger | 0,39 | -0,11 | 0,36 | 0,2 |
| Nile | -0,16 | -0,59 | 0,25 | 0,14 |
| Ob | -0,23 | -0,26 | 0,2 | -0,12 |
| Parana | -0,04 | -0,46 | 0,77 | 0,35 |
| Volga | -0,11 | -0,1 | 0,41 | 0,02 |
| Yangtze | -0,11 | -0,44 | 0,6 | 0,07 |
| Yenisey | -0,18 | -0,05 | 0,38 | 0,04 |

| Basin | GRACE vs. | | | |
|-------------|-----------|------|----------|------|
| | GLDAS | LaD | ORCHIDEE | WGHM |
| Amazon | 0,8 | 0,65 | 0,46 | 0,78 |
| Amur | 0,61 | 0,59 | 0,4 | 0,42 |
| Brahmaputra | 1,46 | 1,47 | 1,65 | 1,3 |
| Congo | 0,5 | 0,58 | 0,5 | 0,55 |
| Danube | 0,99 | 0,97 | 0,6 | 0,7 |
| Ganges | 0,66 | 0,97 | 0,71 | 0,71 |
| Hwang Ho | 0,43 | 0,5 | 0,42 | 0,36 |
| Mekong | 0,53 | 0,49 | 0,75 | 0,6 |
| Mississippi | 0,48 | 0,49 | 0,29 | 0,32 |
| Niger | 0,45 | 0,95 | 0,55 | 0,67 |
| Nile | 0,48 | 0,49 | 0,29 | 0,64 |
| Ob | 0,75 | 0,94 | 0,34 | 0,82 |
| Parana | 0,46 | 0,66 | 0,53 | 0,47 |
| Volga | 0,99 | 0,9 | 0,55 | 0,85 |
| Yangtze | 0,53 | 0,51 | 0,53 | 0,41 |
| Yenisey | 0,75 | 0,73 | 0,5 | 0,75 |

Table 1 (continued)

| RMS (mm/day) | | GRACE vs. | | | |
|--------------|-------------|-------------|--|-------------|-------------|
| Runoff | GLDAS | LaD | | ORCHIDEE | WGHM |
| WGHM | 0,48 | 0,49 | | 0,29 | 0,32 |
| LaD | 0,53 | 0,53 | | 0,33 | 0,35 |
| <i>WGHM</i> | <i>0,8</i> | <i>0,65</i> | | <i>0,46</i> | <i>0,6</i> |
| <i>LaD</i> | <i>0,91</i> | <i>0,64</i> | | <i>0,6</i> | <i>0,77</i> |

Figure caption

Figure 1: Global distribution of the 16 drainage basins chosen in this study: (1: Mississippi, 2: Amazon, 3: Parana, 4: Danube, 5: Niger, 6: Nile, 7: Congo, 8: Volga, 9: Ob, 10: Ganges, 11: Brahmaputra, 12: Yenisey, 13: Amur, 14: Huang Ho, 15: Yangtse, 16: Mekong).

Figure 2a-b: Time series of the ET rate for the sixteen drainage basins, that were computed from the land waters GRACE solutions (Ramillien et al., 2005a) at the resolution of ~660 km (max. harmonic degree = 25-30), and combining with precipitation (GPCC) and runoff data (here WGHM) for the same months. Our GRACE-based estimates are plotted in black, ET profiles from WGHM in red, ORCHIDEE in dark blue, GLDAS in green, LaD in light blue. Results of the statistical comparison are presented on Table 1.

Figure 3 a-b: Time series of the variations of the ET rate over (a) the Amazon basin and (b) the Mississippi basin, considering runoff data from different global models: solid line: using R from WGHM model; dashes line: using R from LaD model.

Figure 4 a-b: Time variations of the regional uncertainties on ET estimates over the basin of (a) the Amazon River and (b) the Mississippi, for different *relative errors on the runoff data*: $\varepsilon_R=5\%$ (blue), 15% (red), 25% (green) and 30% (black).

Figure 1

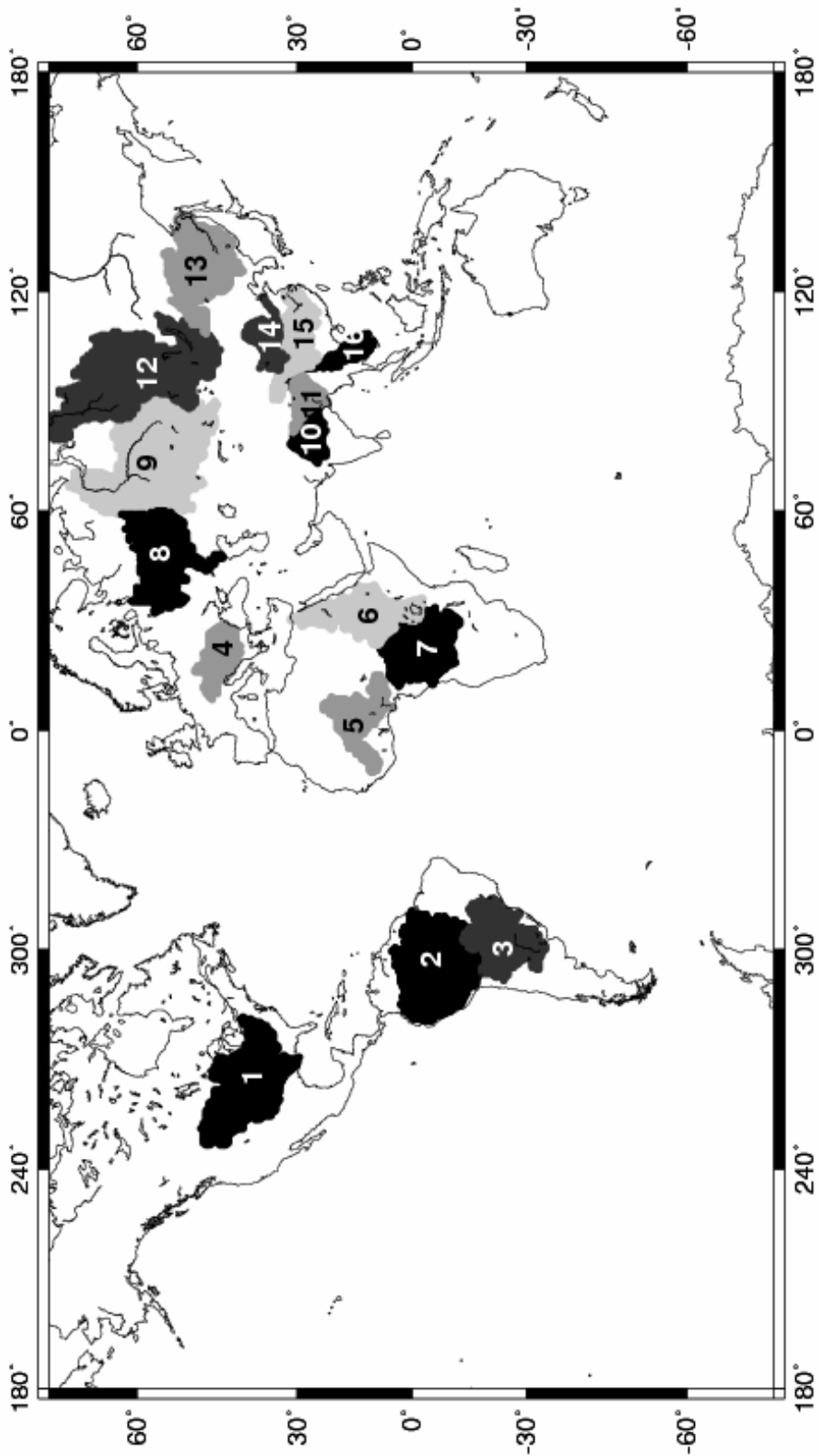


Figure 2a

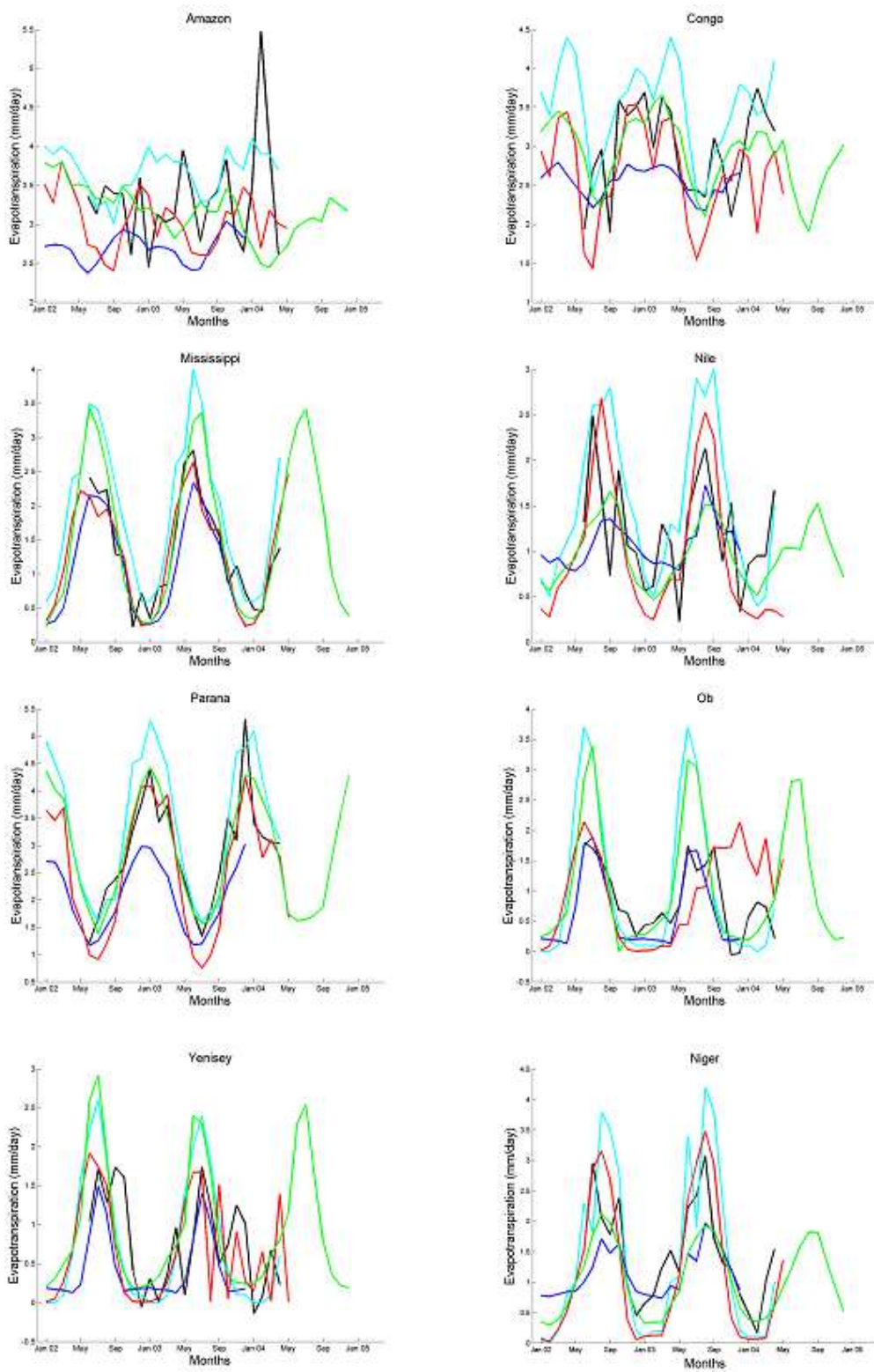


Figure 2b

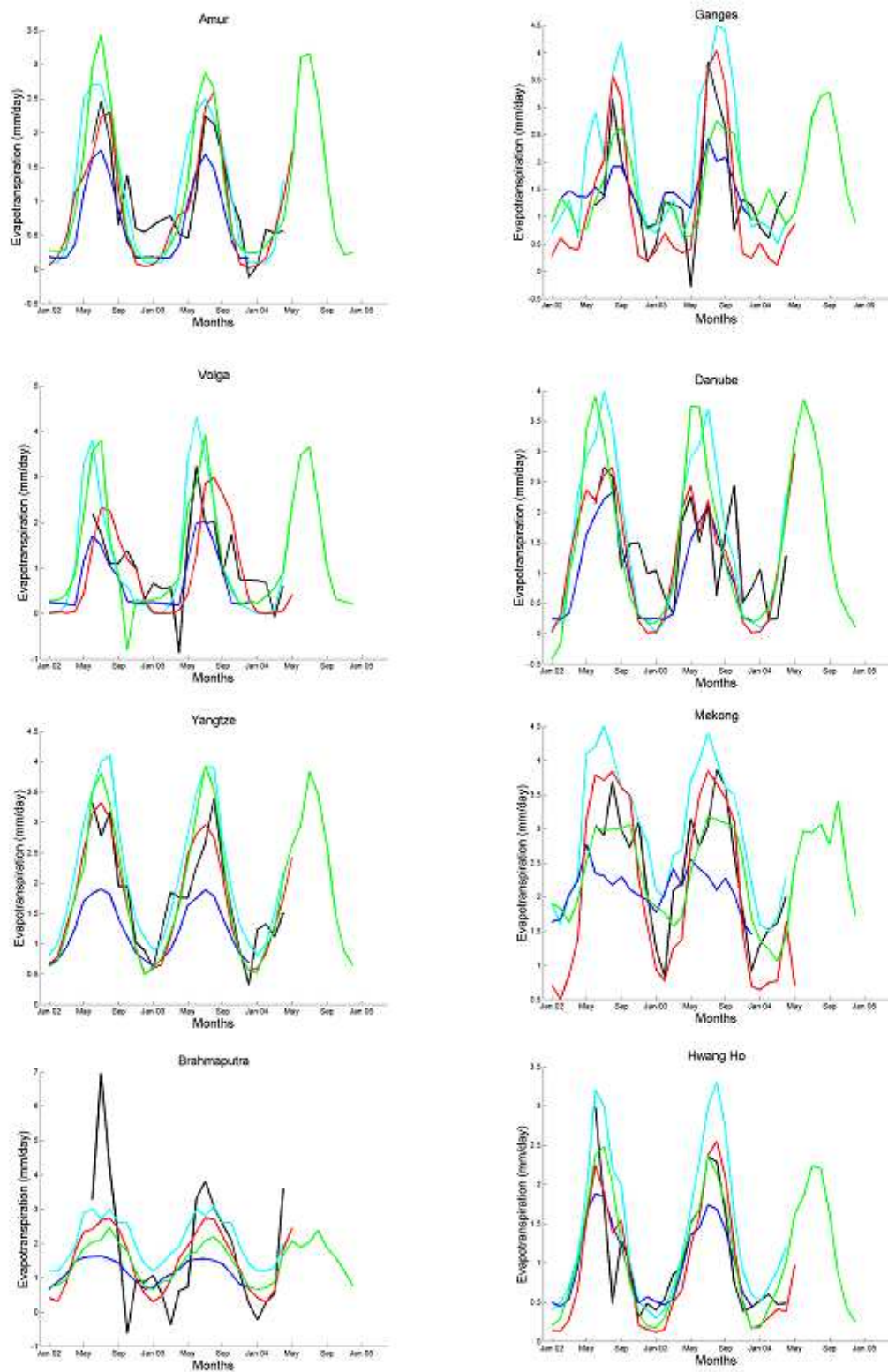


Figure 3a

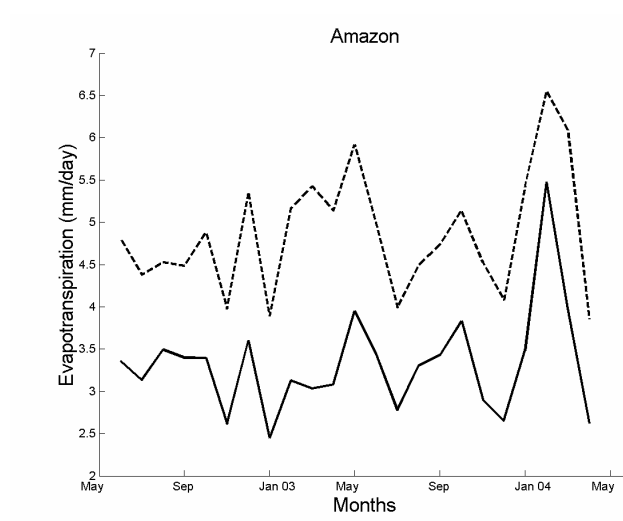


Figure 3b

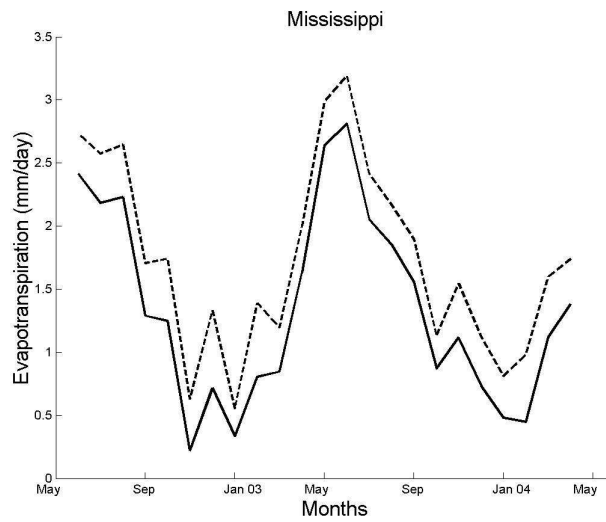


Figure 4a

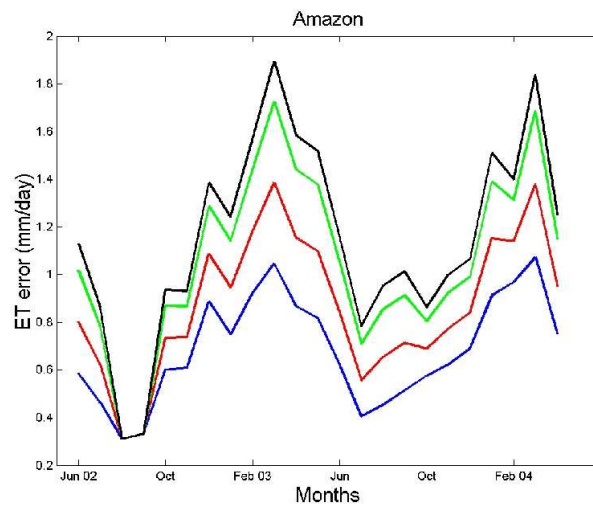


Figure 4b

